

Investigation on Characteristics of 3–5 μm Mid-Infrared Optical Parametric Amplification in LiInS₂

Jingjing Zhang , Feng Yang , Yuanzhai Xu, Hongwei Gao, and Yong Bo

Abstract—The optical parametric amplification process in the mid-infrared (MIR) 3–5 μm region of nonlinear crystal LiInS₂ (LIS) has been investigated. The LIS crystal was pumped by a 1064 nm laser with a pulse width of 30 picoseconds and seeded by a tunable laser generated from a KTP-OPG/OPA pumped by the second harmonic (SH) of the same 1064 nm laser. In the experiment, the 3.28–5.50 μm tunable idler was realized. When the fixed pump energy is 8.75 mJ, the idler energy obtained is 72.2 μJ at 3.28 μm and 63.3 μJ at 5.50 μm . The maximum idler energy of 179.4 μJ at 4.70 μm is reached at a pump energy of 12.5 mJ, and the optimal photon conversion efficiency is 6.36% at the pump energy of 11.5 mJ. Finally, the optical parametric frequency conversion parameters and performance in the 3–5 μm of several typical new crystals (BGSe, LISe, AGS, HGS, and LGS) developed in recent years are briefly compared and summarized.

Index Terms—LiInS₂ crystal, mid-infrared, optical parametric amplifier.

I. INTRODUCTION

UNABLE mid-infrared (MIR) laser sources in the 3–5 μm range are urgently needed for a variety of applications such as remote sensing and aerospace. With the frequency down-conversion technique in nonlinear optics crystals (NLCs), especially using the well-established $\sim 1 \mu\text{m}$ pump source, it is possible to generate laser that emits atmospheric transparency band II (3–5 μm) [1]. One of the core components is infrared NLCs, the desirable properties for targeting crystals are large nonlinear coefficients, wide transparency range, and high laser damage threshold (LDT) [2]. Although many oxide-based crystals (KTP, KTA, PPLN, etc.) are capable of achieving laser in the 3–5 μm . However, the performance of oxide-based crystals from about 4 μm is affected by multi-phonon absorption, making it necessary to use non-oxide materials such as mono-, binary,

Manuscript received 10 June 2024; revised 30 June 2024; accepted 1 July 2024. Date of publication 4 July 2024; date of current version 16 September 2024. This work was supported by the National Natural Science Foundation of China under Grant 61875208. (*Corresponding author:* Feng Yang.)

Jingjing Zhang is with the Key Lab of Solid State Laser, Technical Institute of Physics and Chemistry, Chinese Academy of Sciences, Beijing 100190, China, and also with the University of Chinese Academy of Sciences, Beijing 100049, China (e-mail: vivian0921@163.com).

Feng Yang, Yuanzhai Xu, Hongwei Gao, and Yong Bo are with the Key Lab of Solid State Laser, Technical Institute of Physics and Chemistry, Chinese Academy of Sciences, Beijing 100190, China (e-mail: yang12345yang@163.com; xuyuanzhai@mail.ipc.ac.cn; gaohongwei@mail.ipc.ac.cn; boyong@mail.ipc.ac.cn).

Digital Object Identifier 10.1109/JPHOT.2024.3422989

ternary and quaternary phosphides, arsenides, or chalcogenides (sulfides, selenides and tellurides) [1]. In terms of the growth and processing process as well as physical and optical properties, studies have shown that the main ones that can effectively produce 3–5 μm pumped by $\sim 1 \mu\text{m}$ laser are AgGaS₂ (AGS) [3], [4], [5], BaGa₄Se₇ (BGSe) [2], [6], [7], [8], [9], [10], [11], LiGaS₂ (LGS) [12], [13], Hg₂GaS₄ (HGS) [14], [15], [16], and LiInSe₂ (LISe) [17], [18], [19], [20], [21], [22].

Boyd and colleagues briefly studied the linear and nonlinear properties of LiInS₂ (LIS) in the early 1970s [23]. The large single crystal of LIS grown by Russian scientists using the Bridgman–Stockbarger method for the first time [24]. LIS has a larger band gap than AGS, which is favorable for increasing the LDT, and the bandgap wavelength requirement of $\lambda_g < 500 \text{ nm}$ is necessary to avoid two-photon absorption (TPA) when pumped with $\sim 1 \mu\text{m}$ pump source [18]. In 2001, the nonlinear properties of LIS were determined, and 4.8–9 μm idler was generated [25], [26]. Tao's group started the research on the synthesis and growth of LIS in 2004, the synthesis quality and efficiency of LIS were improved [27]. In 2005, continuous wave differential-frequency generation (CW-DFG) was realized in LIS, and a wide spectral coverage of 5.5–11.3 μm was obtained [28]. In 2020, nanosecond (ns) MIR lasers with narrow linewidths of 6.73–6.84 μm were output in a DFG experiment based on the LIS crystal [29]. However, there is no report on 3–5 μm generation with LIS up to now.

In this article, we have investigated the performance of LIS crystal in the 3–5 μm range using the frequency down-conversion technique pumped by a picosecond (ps) 1064 nm laser. The 3.28–5.50 μm idler laser was experimentally realized. A maximum pulse energy of 179.4 μJ at 4.70 μm was obtained. Moreover, the type-II (e → o + e) phase matching (PM) angles of LIS in the range of 3.28–5.50 μm were experimentally measured and compared with theoretical simulation results. By comparing some of the parameters and PM curves of BGSe, LISe, LIS, AGS, LGS, and HGS, we can further understand the characteristics of LIS crystal and expand its effective applications.

II. EXPERIMENTAL SETUP

The LIS-OPA experimental layout is sketched in Fig. 1, which is also used in LISe and BGS before [22], [30]. This study investigated the optical parametric amplification performance of 3–5 μm in the LIS crystal. A mode-locked Nd: YAG laser

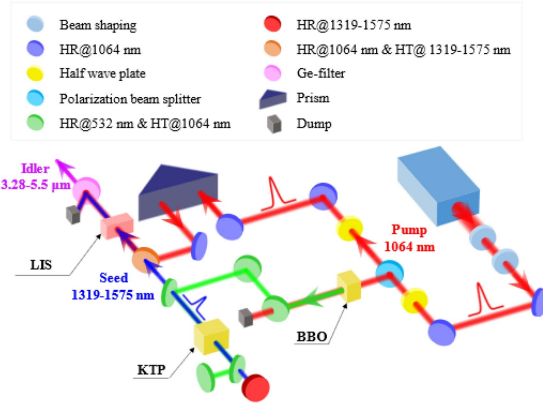
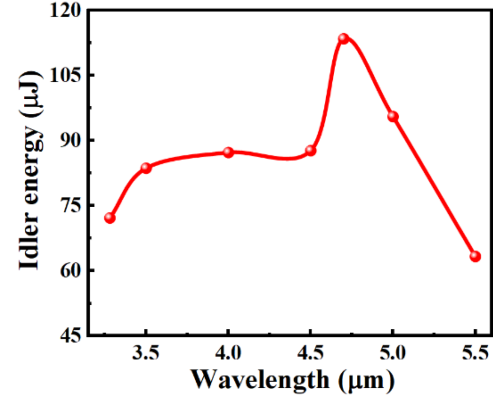


Fig. 1. Experimental setup of the LIS-OPA.

system (EKSPLA: PL2251A) was used as the pump source. The pump wavelength is $\lambda_p = 1064$ nm and the pulse duration is $\tau = 30$ ps, with a repetition frequency set to $f = 10$ Hz. The pump beam diameter was reimaged by a 2:1 telescope from 10 mm to 5 mm. Then the pump laser was split into two energy-adjustable branches using a combination of the half-wave plate (HWP) and polarization beam splitter (PBS) by changing the polarization of pump. The idler generated from the double-pass KTP-OPG/OPA is used as a seed, which can be tuned by rotating KTP and energy-adjusted by controlling the ratio of the pump. The transmitted 1064 nm beam with an adjustable energy via a suitable time delay was used as the pump for the OPA. The time delay controlling of the pump is realized by compensating the optical path difference between the pump and the seed through a prism. Optimal time matching is achieved by slightly adjusting the prism position and observing the idler energy. The pump beam is collimated and mixed with the seed beam through the dichroic mirror and enter the LIS with the same beam diameter. We achieve transverse mode matching by positioning the diaphragm so that the centers of the two beams overlap. Subsequently, the pump is fine-tuned to achieve optimal idler energy. The LIS crystal is mounted on a rotating bracket that is used to calibrate the internal φ angle for PM. The Ge-filter is used to sort out the residual pump and the amplified signal from the idler as much as possible. A thermoelectric energy sensor (OPHIR, PE10-C) was used to detect the idler energy. In addition, since the spectrometer for MIR at 10 Hz is difficult to acquire, we measured the signal wavelength and determine the idler wavelength based on the law of conservation of energy.

LIS has a Wurtzite-type ($\beta\text{-NaFeO}_2$) structure. It belongs to the orthorhombic symmetry of the $mm2$ point group. LIS is a negative biaxial crystal, at longer wavelengths it can be regarded as quasi-uniaxial [17]. And the LIS sample used in our experiment were tested to have an absorption coefficient of 0.46 cm^{-1} . In 2014, new Sellmeier equation for LIS were reported, and the PM characteristics can be calculated by (where the wavelength λ is in micrometers) [31]:

$$n_x^2 = 6.70276 + \frac{0.13853}{\lambda^2 - 0.05712} + \frac{2164.01}{\lambda^2 - 942.06}$$

Fig. 2. The wavelength dependence of the idler from 3.28 to 5.50 μm for LIS-OPA at a fixed pump energy of 8.8 mJ.

$$\begin{aligned} n_y^2 &= 7.09598 + \frac{0.14240}{\lambda^2 - 0.06514} + \frac{2511.13}{\lambda^2 - 988.03} \\ n_z^2 &= 7.55716 + \frac{0.15063}{\lambda^2 - 0.06604} + \frac{3241.54}{\lambda^2 - 1090.62} \end{aligned} \quad (1)$$

We calculated the PM curve of LIS crystal at pump wavelength of 1064 nm using (1). Subsequently, the sample employed in the experiment was cut in the X-Y plane at $\theta = 90^\circ$, $\varphi = 45^\circ$ for type-II interactions with a maximum effective nonlinearity $d_{eff} = 6.5 \text{ pm/V}$. The LIS sample is $6.5 \text{ mm} \times 5 \text{ mm}$ in aperture and 4 mm along the propagation direction. The wider transverse aperture of 6 mm is engineered to extend the angular adjustment range for PM. At the same time, optically polished in both end faces without coating.

III. RESULTS AND DISCUSSION

The wavelength dependence of the idler was investigated by simultaneously tuning the seed wavelength and the incidence angle of the LIS crystal to satisfy the PM conditions. At a fixed pump energy of 8.75 mJ, the idler energy versus MIR wavelength plotted in Fig. 2. The system could deliver a maximum idler energy of $113.5 \mu\text{J}$ at $4.70 \mu\text{m}$, the characteristic enhancement at normal incidence due to the attenuated Fresnel losses. The tuning range from 3.28 to $5.50 \mu\text{m}$ was obtained. The absorption by atmospheric molecules (such as water) contributes to the reduction at $4.0\text{--}4.5 \mu\text{m}$ and $5.50 \mu\text{m}$, the decrease in long wavelength is associated with a decrease in parametric gain. LIS crystal can't achieve higher conversion efficiency than BGSe, which is related to the difference of the nonlinear coefficients [32]. In addition, by further increasing the pump energy and optimizing the crystal length, LIS is expected to generate higher energy than LiSe after $4.70 \mu\text{m}$ [22]. Meanwhile, we measured the PM angle of LIS-OPA. It can be seen in Fig. 4 that the experimental data of LIS-OPA are in good agreement with the calculations based on the Sellmeier equation in [31].

In the experiment, the idler wavelength is $4.70 \mu\text{m}$ at the normal incidence, we investigated the effect of the seed level on the idler energy, and the seed energy was kept at $200 \mu\text{J}$.

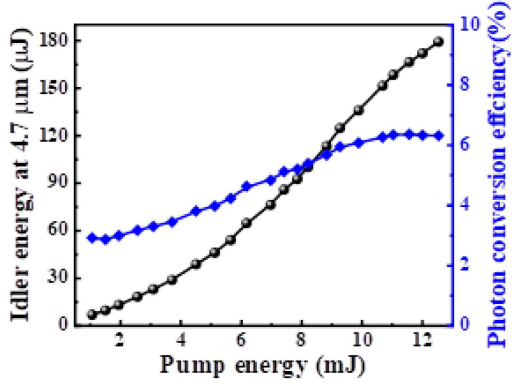


Fig. 3. Idler energy of the LIS-OPA at 4.7 μm (normal incidence, $\theta = 90^\circ$, $\varphi = 45^\circ$) versus pump energy at 1064 nm.

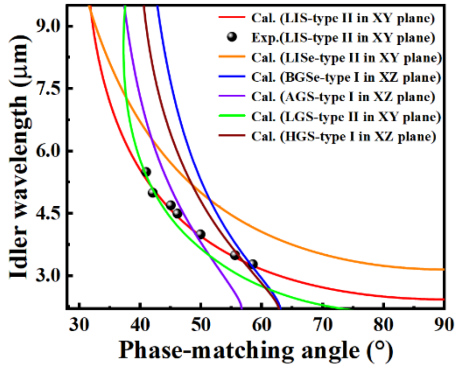


Fig. 4. Tuning wavelength of the OPA versus internal angle. Symbols are experimental data of LIS-OPA and curves are simulation results of LIS, LISe, BGSe, AGS, LGS, and HGS.

Fig. 3 shows the idler energy at 4.70 μm versus the pump energy, corresponding to the signal wavelength of 1375 nm. It can be seen from Fig. 3 that the idler energy increases monotonically with the pump energy. The optimized pump-to-idler photon conversion efficiency was 6.36%, under the pump energy of 11.5 mJ, after which the conversion efficiency saturates. This may be because the parametric gain of 4 mm LIS crystal is close to saturation. At the maximum pump energy of 12.5 mJ, the highest idler energy of 179.4 μJ was obtained. Since the LIS crystal was not coated, the Fresnel loss was considered.

In addition, Table I shows a comparison of the parameters of some NLCs that have achieved continuously 3–5 μm using 1 μm pump in recent years. AGS has the lowest residual absorption, but due to the poor thermal conductivity, low LDT, and thermal expansion anisotropy, which leads to thermo-mechanical stresses and is significant at high pump level, it is not suitable for high repetition frequency and high energy [3], [4], [5]. In general, Ba compounds have a wider band gap than Ag compounds. Usually, this is associated with higher damage resistivity, hardness and thermal conductivity. In recent years of research, BGSe have shown great potential for MIR generation, the tuning range covers the entire MIR band at a low repetition frequency. However, limited by the low thermal conductivity, the research under high repetition frequency and high average

TABLE I
COMPARISON OF CRYSTAL PARAMETERS WHICH HAVE ACHIEVED TUNED 3–5 μm BASED ON 1 μm PUMP

| | Transmission range / μm | Band gap / eV | Nonlinear coefficient / $\text{pm} \cdot \text{V}^{-1}$ | Thermal conduct. / $\text{W} \cdot \text{mK}^{-1}$ |
|------|------------------------------------|---------------|---|--|
| AGS | 0.47–13 | 2.76 | $d_{32} = 8$ $d_{36} = 19$ | 1.5 |
| BGSe | 0.47–18 | 2.64 | $d_{11} = 24.3$ $d_{13} = 20.4$ | 0.56–0.74 |
| LGS | 0.32–11.6 | 4.15 | $d_{31} = 5.8$ $d_{23} = 5.1$ | 6–8 |
| HGS | 0.55–13 | 2.79 | $d_{36} = 27.2$ | 2.31–2.36 |
| LISe | 0.45–14 | 2.86 | $d_{33} = 16$ | 5 |
| LIS | 0.34–13.2 | 3.59 | $d_{31} = 7.2$ $d_{32} = 5.3$ | 7.6 |

pump power is still in exploratory stage. When the 1064 nm is utilized as the pump, the repetition frequency of the pump laser in existing reports is generally below 1 kHz [2], [6], [7], [8], [33], [10], [11]. For LGS crystal, which have high LDT and thermal conductivity, many MIR generated under kHz or MHz pump have been reported, and the large bandgap makes it suitable for using 1 μm pump. However, due to its small geometrical size, the gain length is shorter under ns pump condition, resulting in lower idler energy. In addition, LGS has an obvious absorption peak near 8 μm , the transmittance decreases significantly, which makes it unsuitable for LWIR generation [12], [13]. HGS competes directly with AGS because the similar transparency windows. It has a significant advantage over the AGS due to a nonlinear coefficient d_{36} that is about 1.8 times higher. Also, the band gap of HGS is slightly increased compared to AGS, which results in a slight increase in the damage resistivity. However, due to the presence of multiple phases in HGS, oriented seeds cannot be used, making it difficult to grow large sizes [14], [15], [16]. The transmission range of LIS is 0.34–13.2 μm , which has a shorter upper limit than that of BGSe (0.47–18 μm), LISe (0.45–13.7 μm), AGS (0.47–13 μm), and HGS (0.55–13 μm). Therefore, LIS is conducive to using the well-established 1 μm pump source and frequency down-conversion technology to obtain the MIR radiation. LISe has a higher nonlinear coefficient than LIS and has a higher conversion efficiency when used for MIR generation [24], [25], [26], [31], [33], [34], [35]. Despite the low idler energy achieved at this stage, both LIS and LISe have the potential to be applied for high repetition frequency and high power due to their high thermal conductivity and low thermo-optic coefficient [18], [19], [20], [21], [22]. In conclusion, optimizing the optical quality of NLCs as well as improving the performance of the pump source has the great impact on enhancing the performance of MIR laser.

Furthermore, we have plotted the PM curves of LIS (type-II in XY plane), LISe (type-II in XY plane), BGSe (type-I in XZ plane), AGS (type-I in XZ plane), LGS (type-II in XY plane), and HGS (type-I in XZ plane) in Fig. 4. It should be noted that the PM type chosen in the simulation is the one which they can generate 3–5 μm with the maximum d_{eff} . The pump was selected as 1064 nm based on the experimental program. The curves of tuning angle versus parametric wavelength were theoretically compared. In comparison, BGSe can realize wider idler with the

narrowest angular range. Theoretical simulations show that LIS has an advantage in generating 3–5 μm MIR radiation compared to LiSe, which is unable to achieve laser output below 3.2 μm . In fact, in the previous study of LiSe using this system, the idler wavelength range achieved was 3.6–4.8 μm [22].

IV. CONCLUSION

In summary, we investigate the performance of LIS crystal in the 3–5 μm range using frequency down-conversion technique with ps 1064 nm pump source. Under a fixed pump energy of 8.75 mJ, the idler energy is 72.2 μJ at 3.28 μm and 63.3 μJ at 5.50 μm . Moreover, the maximum idler energy at 4.7 μm was obtained to be 179.4 μJ under a pump energy of 12.5 mJ, and the optimized pump-to-idler photon conversion efficiency is 6.36%. Some parameters and PM curves of LIS, BGSe, LiSe, AGS, and LGS are compared, and the advantages and bottlenecks of them are further summarized. With the improved optical quality of the LIS crystal and further experimental optimization, it is attractive for OPAs and OPOs pumped by established high-power $\sim 1 \mu\text{m}$ lasers for generating MIR.

ACKNOWLEDGMENT

The authors would like to thank the support of LIS crystal from State Key Laboratory of Crystal Materials, Shandong University.

REFERENCES

- [1] V. Petrov, “Frequency down-conversion of solid-state laser sources to the mid-infrared spectral range using non-oxide nonlinear crystals,” *Prog. Quantum Electron.*, vol. 42, pp. 1–106, Jul. 2015.
- [2] X. Zhang, J. Y. Yao, W. L. Yin, Y. Zhu, Y. C. Wu, and C. T. Chen, “Determination of the nonlinear optical coefficients of the BaGa₄Se₇ crystal,” *Opt. Exp.*, vol. 23, no. 1, pp. 552–558, Jan. 2015.
- [3] T. J. Wang et al., “Wide-tunable, high-energy AgGaS₂ optical parametric oscillator,” *Opt. Exp.*, vol. 14, no. 26, pp. 13001–13006, Dec. 2006.
- [4] W. Harmon, K. Robben, and C. M. Cheatum, “Adding a second AgGaS₂ stage to Ti:Sapphire/BBO/AgGaS₂ setups increases mid-infrared power twofold,” *Opt. Lett.*, vol. 48, no. 18, pp. 4797–4800, Sep. 2023.
- [5] K. L. Vodopyanov, J. P. Maffetone, I. Zwieback, and W. Ruderman, “AgGaS₂ optical parametric oscillator continuously tunable from 3.9 to 11.3 μm ,” *Appl. Phys. Lett.*, vol. 75, no. 9, pp. 1204–1206, Aug. 1999.
- [6] Y. C. Zhang, Y. Zuo, Z. Li, B. Wu, J. Y. Yao, and Y. H. Shen, “High energy mid-infrared laser pulse output from a BaGa₄Se₇ crystal-based optical parametric oscillator,” *Opt. Lett.*, vol. 45, no. 16, pp. 4595–4598, Aug. 2020.
- [7] J. Y. Yao et al., “BaGa₄Se₇: A new congruent-melting IR nonlinear optical material,” *Inorganic Chem.*, vol. 49, no. 20, pp. 9212–9216, Oct. 2010.
- [8] J. Y. Yao et al., “Growth and characterization of BaGa₄Se₇ crystal,” *J. Cryst. Growth*, vol. 346, no. 1, pp. 1–4, 2012.
- [9] Y. He et al., “Intracavity-pumped, mid-infrared tandem optical parametric oscillator based on BaGa₄Se₇ Crystal,” *IEEE Photon. J.*, vol. 11, no. 6, Dec. 2019, Art. no. 1300109.
- [10] A. P. Yelisseyev, S. I. Lobanov, P. G. Krinitin, and L. I. Isaenko, “The optical properties of the nonlinear crystal BaGa₄Se₇,” *Opt. Mater.*, vol. 99, Jan. 2020, Art. no. 109564.
- [11] N. Y. Kostyukova et al., “Widely tunable in the mid-IR BaGa₄Se₇ optical parametric oscillator pumped at 1064 nm,” *Opt. Lett.*, vol. 41, no. 15, pp. 3667–3670, Aug. 2016.
- [12] T. H. Ma, C. H. Yang, L. Sun, C. Xu, and Y. F. Chen, “Synthesis and characterization of orthorhombic LiGaS₂,” *Mater. Sci. Technol.*, vol. 20, no. 3, pp. 121–126, 2012.
- [13] S. N. Smetanin et al., “50 μJ level, 20 picosecond, narrowband difference-frequency generation at 4.6, 5.4, 7.5, 9.2, and 10.8 μm in LiGaS₂ and LiGaSe₂ at Nd:YAG laser pumping and various crystalline Raman laser seedings,” *Opt. Mater. Exp.*, vol. 10, no. 8, pp. 1881–1890, Aug. 2020.
- [14] B. Levine, C. Bethea, H. Kasper, and F. Thiel, “Nonlinear optical susceptibility of HgGa₂S₄,” *IEEE J. Quantum Electron.*, vol. QE-12, no. 6, pp. 367–368, Jun. 1976.
- [15] V. Petrov, “Parametric down-conversion devices: The coverage of the mid-infrared spectral range by solid-state laser sources,” *Opt. Mater.*, vol. 34, no. 3, pp. 536–554, Jan. 2012.
- [16] A. Tyazhev et al., “High-power HgGa₂S₄ optical parametric oscillator pumped at 1064nm and operating at 100 hz,” *Laser Photon. Rev.*, vol. 7, no. 4, pp. L21–L24, Jul. 2013.
- [17] S. Fossier et al., “Optical, vibrational, thermal, electrical, damage, and phase-matching properties of lithium thioindate,” *J. Opt. Soc. Amer. B*, vol. 21, no. 11, pp. 1981–2007, Nov. 2004.
- [18] L. Isaenko et al., “Characterization of LiInS₂ and LiInSe₂ single crystals for nonlinear optical applications,” in *Proc. Conf. Prog. Semicond. Mater. Optoelectron Appl. MRS Fall Meeting*, Boston, MA, USA, 2001, vol. 692, pp. 429–434.
- [19] J. J. Zondy, V. Vedenyapin, A. Yelisseyev, S. Lobanov, L. Isaenko, and V. Petrov, “LiInSe₂ nanosecond optical parametric oscillator,” *Opt. Lett.*, vol. 30, no. 18, pp. 2460–2462, Sep. 2005.
- [20] V. Petrov et al., “Optical, thermal, electrical, damage, and phase-matching properties of lithium selenoindate,” *J. Opt. Soc. Amer. B*, vol. 27, no. 9, pp. 1902–1927, Sep. 2010.
- [21] J. J. Zondy, V. Petrov, A. Yelisseyev, L. Isaenko, and S. Lobanov, “Orthorhombic crystals of lithium thioindate and selenoindate for nonlinear optics in the mid-IR,” in *Proc. NATO Adv. Res. Workshop Mid-Infrared Coherent Sources*, Barcelona, Spain, 2008, pp. 67–104.
- [22] S. B. Dai et al., “Picosecond mid-infrared optical parametric amplifier based on LiInSe₂ with tenability extending from 3.6 to 4.8 μm ,” *Opt. Exp.*, vol. 25, no. 11, pp. 12860–12866, 2017.
- [23] G. D. Boyd, H. M. Kasper, and J. H. McFee, “Linear and nonlinear optical properties of LiInS₂,” *J. Appl. Phys.*, vol. 44, no. 6, pp. 2809–2812, 1973.
- [24] L. Isaenko et al., “Growth and characterization of LiInS₂ single crystals,” *J. Cryst. Growth*, vol. 218, no. 2–4, pp. 313–322, Sep. 2000.
- [25] L. Isaenko et al., “LiInS₂: A new nonlinear crystal for the mid-IR,” *Mater. Sci. Semicond. Process.*, vol. 4, no. 6, pp. 665–668, Dec. 2001.
- [26] F. Rotermund, V. Petrov, F. Noack, L. Isaenko, A. Yelisseyev, and S. Lobanov, “Optical parametric generation of femtosecond pulses up to 9 μm with LiInS₂ pumped at 800 nm,” *Appl. Phys. Lett.*, vol. 78, no. 18, pp. 2623–2625, Apr. 2001.
- [27] S. P. Wang, X. T. Tao, G. D. Liu, C. M. Dong, and M. H. Jiang, “Study on the growth and properties of large infrared nonlinear optical crystal LiInS₂,” *J. Synthetic Crystals*, vol. 38, no. 4, pp. 851–855, 2009.
- [28] W. D. Chen et al., “Widely tunable continuous-wave mid-infrared radiation (5.5–11 μm) by difference-frequency generation in LiInS₂ crystal,” *Appl. Opt.*, vol. 44, no. 19, pp. 4123–4129, Jul. 2005.
- [29] L. I. Stoychev et al., “DFG-based mid-IR tunable source with 0.5 mJ energy and a 30 pm linewidth,” *Opt. Lett.*, vol. 45, no. 19, pp. 5526–5529, Oct. 2020.
- [30] J. J. Zhang et al., “Tunable mid-IR optical parametric amplifier pumped at 1064 nm based on a wideband-gap BaGa₄S₇ crystal,” *Infrared Phys. Technol.*, vol. 111, Dec. 2020, Art. no. 103571.
- [31] K. Kato and N. Umemura, “Sellmeier and thermo-optic dispersion formulas for LiInS₂,” *Appl. Opt.*, vol. 53, no. 33, pp. 7998–8001, Nov. 2014.
- [32] F. Yang et al., “High efficiency and high peak power picosecond mid-infrared optical parametric amplifier based on BaGa₄Se₇ crystal,” *Opt. Lett.*, vol. 38, no. 19, pp. 3903–3905, Oct. 2013.
- [33] G. M. H. Knippels et al., “Mid-infrared (2.75–6.0 μm) second-harmonic generation in LiInS₂,” *Opt. Lett.*, vol. 26, no. 9, pp. 617–619, May 2001.
- [34] K. Imasaka, K. Ogawa, N. Ishii, M. Maruyama, and R. Itakura, “Ultra-short near-infrared pulse generation by non-collinear optical parametric amplification in LiInS₂,” *Opt. Continuum*, vol. 1, no. 9, pp. 1956–1962, 2022.
- [35] M. Magesh, A. Arunkumar, P. Vijayakumar, G. A. Babu, and P. Ramasamy, “Growth and characterization of LiInS₂ single crystal by Bridgman technique,” in *Proc. Conf. AIP*, vol. 1536, no. 1, 2013, pp. 357–358.